JAM-A promotes neutrophil chemotaxis by controlling integrin internalization and recycling

Maria Rosaria Cera[1], Monica Fabbri[2], Cinzia Molendini[1], Monica Corada[1], Fabrizio Orsenigo[1], Markus Rehberg[3], Christoph A. Reichel[3], Fritz Krombach[3], Ruggero Pardi[2] and Elisabetta Dejana[1,4,5,*]

[1]FIRC Institute of Molecular Oncology, Milan, Italy
[2]Vita-Salute San Raffaele University and DIBIT San Raffaele Scientific Institute, Milan, Italy
[3]Walter Brendel Center of Experimental Medicine, Ludwig-Maximilians-Universität München, Munich, Germany
[4]Department of Biomolecular Sciences and Biotechnologies, School of Sciences, University of Milan, Milan, Italy
[5]Mario Negri Institute of Pharmacological Sciences, Milan, Italy
*Author for correspondence (e-mail: elisabetta.dejana@ifom-ieo-campus.it)

Accepted 24 October 2008
Journal of Cell Science 122, 268-277 Published by The Company of Biologists 2009
doi:10.1242/jcs.037127

Summary

The membrane-associated adhesion molecule JAM-A is required for neutrophil infiltration in inflammatory or ischemic tissues. JAM-A expressed in both endothelial cells and neutrophils has such a role, but the mechanism of action remains elusive. Here we show that JAM-A has a cell-autonomous role in neutrophil chemotaxis both in vivo and in vitro, which is independent of the interaction of neutrophils with endothelial cells. On activated neutrophils, JAM-A concentrates in a polarized fashion at the leading edge and uropod. Surprisingly, a significant amount of this protein is internalized in intracellular endosomal-like vesicles where it codistributes with integrin β1. Clustering of β1 integrin leads to JAM-A co-clustering, whereas clustering of JAM-A does not induce integrin association. Neutrophils derived from JAM-A-null mice are unable to correctly internalize β1 integrins upon chemotactic stimuli and this causes impaired uropod retraction and cell motility. Consistently, inhibition of integrin internalization upon treatment with BAPTA-AM induces a comparable phenotype. These data indicate that JAM-A is required for the correct internalization and recycling of integrins during cell migration and might explain why, in its absence, the directional migration of neutrophils towards an inflammatory stimulus is markedly impaired.

Supplementary material available online at
http://jcs.biologists.org/cgi/content/full/122/2/268/DC1

Key words: Integrins, JAM, Leukocyte, Chemotaxis

Introduction

JAM-A (also known as F11R or JAM1) was the first member of the junctional adhesion molecule (JAM) family to be discovered. These proteins are small Ig superfamily members displaying two extracellular Ig loops and an intracellular region, which associates via PSD95–Dlg–ZO-1 binding residues to several intracellular partners containing PDZ domains. JAM-A is enriched at endothelial and epithelial tight junctions where it increases cell-cell adhesion through homophilic interactions with JAM-A molecules expressed in the adjacent cells (for reviews, see Bazzoni and Dejana, 2004; Bradfield et al., 2007; Vestweber, 2007; Weber et al., 2007). JAM-A is also present in leukocytes and platelets where it has a role in promoting leukocyte motility and platelet aggregation (Kornecki et al., 1990; Liu et al., 2000). In different experimental systems, both in vitro and in vivo, it was shown that JAM-A is needed for the proper transmigration of leukocytes through endothelial junctions. Deletion of the gene encoding JAM-A or administration of blocking antibodies in vivo strongly reduces neutrophil and monocyte infiltration in a range of inflammatory conditions (for reviews, see Bradfield et al., 2007; Vestweber, 2007; Weber et al., 2007; Del Maschio et al., 1999; Martin-Padura et al., 1998). JAM-A expressed by endothelial cells is responsible for the control of leukocyte transmigration through intercellular junctions (Khandoga et al., 2005; Woodfin et al., 2007). However, in inflammatory peritonitis, as well as in heart ischemia and reperfusion injury, JAM-A expressed on neutrophils also has a role in promoting neutrophil infiltration into inflammatory and ischemic tissues (Corada et al., 2005). JAM-A-null neutrophils frequently become arrested either on the surface of endothelial cells, where they form small aggregates, or at the interface between endothelial cells and the basement membrane, suggesting that, after diapedesis through endothelial cell junctions, they are unable to infiltrate the underlying tissues efficiently.

In the present work, we provide direct in vivo evidence of this hypothesis. We show that once neutrophils have transmigrated across endothelial cells their subsequent capacity to migrate within the interstitial tissue towards a chemotactic stimulus is significantly impaired. We also found that JAM-A could have a permissive role in modulating integrin function in human and mouse neutrophils in vitro. Chemotactic activation of neutrophils induces rapid JAM-A internalization and co-distribution with β1 integrins in endocytic compartments. In the absence of JAM-A the endo-exocytic cycle of integrins is perturbed, resulting in increased surface expression of functionally competent integrins, which promote strong cell adhesion and consequently reduce cell motility. Thus, the effect of JAM-A on integrin internalization might explain the altered cell motility of JAM-A-null neutrophils in vitro as well as in various experimental models in vivo.

Results

In a previous work we presented evidence that JAM-A expression in neutrophils was required for efficient directional migration in vitro (Corada et al., 2005). To extend this observation to an in vivo model, we applied intravital reflected light oblique transillumination

(RLOT) microscopy imaging to visualize and quantify the stepwise transmigration of neutrophils at postcapillary venules in the inflamed mouse cremaster muscle. Tissue distribution of transmigrated leukocytes was quantified in two regions of interest (ROIs), one proximal and one distal to the vessel (Fig. 1A), as described in the Materials and Methods.

As previously shown, in response to 60 minutes of stimulation with leukotriene B4 (LTB4), the total numbers of transmigrated leukocytes did not differ significantly between WT and JAM-A-deficient mice (data not shown) (Woodfin et al., 2007). However, a significantly smaller proportion of transmigrated leukocytes accumulated in the ROI distal to the analyzed postcapillary venule (>25 μm from the venule) in JAM-A-deficient compared with WT mice (Fig. 1B), suggesting that interstitial migration of transmigrated leukocytes in response to LTB4 is impaired in JAM-A-deficient mice.

To decipher the mechanistic role of JAM-A in controlling neutrophil migration, we first asked whether JAM-A presented a polarized distribution in activated HL60 cells. These cells were selected because they are better suited to imaging analysis as than murine neutrophils and are able to polarize quickly upon activation with chemotactic stimuli. HL60 cells express JAM-A, as shown by immunoprecipitation followed by western blot and FACS analysis (supplementary material Fig. S1). When these cells were treated with *N*-formyl-l-methionyl-l-leucyl-l-phenylalanine (fMLP), in maximally polarized cells JAM-A displayed a bipolar localization and codistributed with actin in ruffles at the leading edge and at the uropod (Fig. 2, arrows). In addition, JAM-A was found in intracellular vesicles (Fig. 2, arrowheads). In low or partially polarized cells, JAM-A appeared concentrated in intracellular vesicles variably distributed along the cell body (supplementary material Fig. S2). Untreated cells displayed very few, if any, JAM-A-positive vesicles whereas both fMLP and phorbol 12-myristate 13-acetate (PMA) induced a strong increase in their number (Fig. 3A). In transverse sections, vesicles were distributed in a scattered manner within the cytosol (Fig. 3B). JAM-A-containing vesicles could be detected whether the JAM-A antibodies were added before (Fig. 2) or after (Fig. 3) fixation, excluding a significant contribution of antibody-mediated clustering in JAM-A internalization upon cell activation with chemotactic stimuli. As reported in supplementary material Fig. S3, we noticed that, when staining was performed after fixation, most cells presented an intense JAM-A-positive peripheral rim. When staining was performed before fixation, a significant number of cells did not show a JAM-A-positive peripheral rim (supplementary material Fig. S3, staining of living cells, compare the two types of JAM-A staining). This explains the different JAM-A localization in the peripheral rim of untreated cells comparing staining after fixation (Fig. 3A) with staining before fixation (Fig. 4A).

To further prove the intracellular nature of JAM-A vesicles, pre-cooled HL60 cells were incubated on ice with antibodies against JAM-A for 30 minutes, to allow mAb binding to the cell surface (supplementary material Fig. S4). The unbound antibody was then washed and the cells seeded on fibronectin-coated coverslips and stimulated with fMLP at 37°C for 20 minutes. Surface-bound antibody was stripped by acid washing and cells were fixed with paraformaldehyde and permeabilized with saponin.

As shown in supplementary material Fig. S4, under these conditions several JAM-A-containing vesicles could be found in permeabilized cells (supplementary material Fig. S4f). By contrast, control IgG or an isotype-matched irrelevant mAb were fully washed

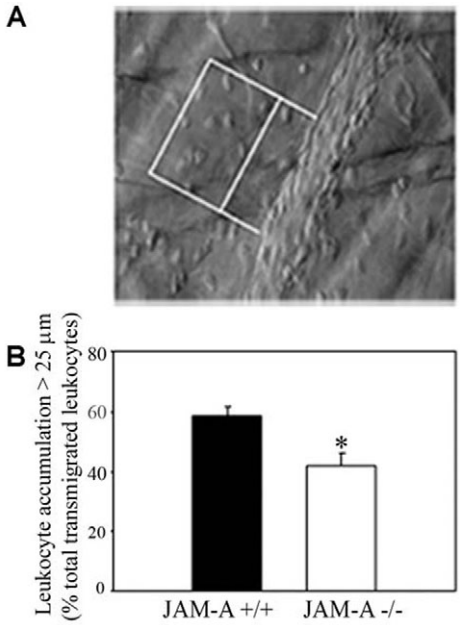

Fig. 1. Impaired interstitial migration of extravasated leukocytes in vivo in JAM-A-deficient mice. (A) In vivo RLOT microscopic image of a postcapillary venule in the inflamed mouse cremaster muscle. Tissue distribution of transmigrated leukocytes was quantified in two regions of interest (ROIs), one close and one distant to the vessel (indicated by the two boxed regions). (B) Quantitative analysis of tissue distribution of transmigrated leukocytes after 60 minutes of stimulation with LTB4. In JAM-A-deficient mice, a significantly smaller proportion (41.9±4.1%) of transmigrated leukocytes is found in the ROI distant to the analyzed postcapillary venule (>25 μm distance from the venule) compared with a similar region in JAM-A$^{+/+}$ mice (58.5±3.1%; n=6; mean ± s.e.m.; *P<0.05 vs JAM-A$^{+/+}$).

out, showing the specific nature of the internalized vesicles (supplementary material Fig. S4d,e).

We then extended the study to freshly isolated human neutrophils. As reported in Fig. 4A, following fMLP stimulation, JAM-A was found in endocytic vesicles, in a similar localization to that observed in HL60 cells. To quantify fMLP-mediated JAM-A internalization, neutrophils were labeled at 4°C with a cleavable biotin and then treated or not with fMLP (100 nM for 5 minutes at 37°C). After this procedure, biotin was cleaved with the non-membrane-permeable reducing agent glutathione (GSH) and cells were lysed. The biotinylated internalized JAM-A was then precipitated with streptavidin-agarose and revealed with anti-JAM-A. As a control, the same blot was immunolabeled with anti-αL-integrin mAb. As reported in Fig. 4B-C, upon fMLP treatment, JAM-A internalization was enhanced compared with that in untreated cells with a kinetics similar to αL integrin. As expected, αL integrin internalization peaks at 5 minutes after stimulation, as previously reported (Fabbri et al., 2005).

In a previous work (Corada et al., 2005), we showed that adhesion and spreading of JAM-A-null neutrophils to fibronectin, laminin and ICAM-1 (intercellular adhesion molecule 1) was increased compared with levels in JAM-A-positive cells. Furthermore, in the absence of JAM-A, neutrophils were unable to retract the uropod, and showed abnormally elongated tails. These observations suggest that JAM-A might interact with integrins and influence their activity, as well as their turnover. Consistently with this hypothesis, we observed a striking codistribution of integrin β1, β2 and α5 in

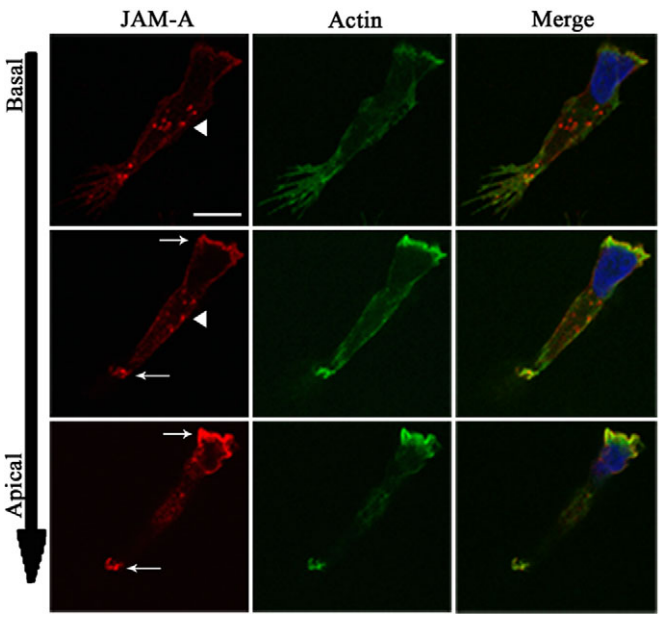

Fig. 2. JAM-A distribution in polarized dHL60 cells. Confocal immunofluorescence analysis of polarized dHL60 (fMLP stimulation for 20 minutes). Double staining for JAM-A (red) and actin (green) is shown. The anti-JAM-A mAb was applied to living cells before paraformaldehyde fixation (see Materials and Methods). Cell nuclei were counterstained with DAPI (blue). The image represents the *z*-stack projection of 25 confocal sections from the basal to the apical cell side, as indicated by the arrow on the left (stack *z*-spacing, 2 μm). JAM-A is localized in intracellular vesicles (arrowheads), at the uropod and in ruffles at the leading edge (arrows). Scale bar: 5 μm.

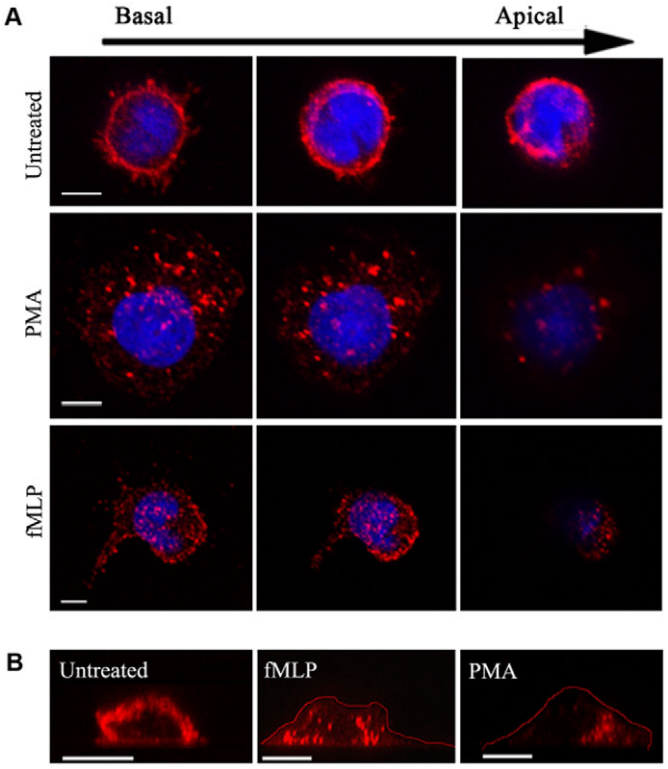

Fig. 3. JAM-A is internalized in polarized dHL60 cells. (A) Cells were seeded on fibronectin-coated coverslips, then treated or not with fMLP or PMA for 20 minutes, fixed with paraformaldehyde and stained for JAM-A (red). The nuclei of the cells were counter-stained with DAPI (blue). JAM-A is distributed in intracellular vesicles in activated cells, as shown by the confocal z-stack projections from the basal to the apical side of the cell (from the left to the right, as indicated by the arrow on the top). (B) Corresponding lateral view of JAM-A distribution in intracellular vesicles along the cell body. The images represent the maximum projection along the *xz* axes of confocal stacks of about 15 sections (stack *z*-spacing, 0.4 μm). Scale bars: 5 μm.

JAM-A-positive intracellular vesicles (Fig. 5). To further investigate the reciprocal interaction between integrins and JAM-A in unfixed cells, we incubated adherent neutrophils with fibronectin-coated beads. We found that both β1 integrin and JAM-A promptly co-clustered at the site of bead adhesion (Fig. 6). The clustering was specific, because polylysine-coated beads were ineffective (Fig. 6; supplementary material Fig. S5) and MHC Class I, a membrane protein that can undergo recycling, did not cluster around fibronectin- or polylysine-coated beads (supplementary material Fig. S5). Furthermore, beads coated with antibodies against β1 integrin were able to induce the co-clustering of JAM-A. Conversely, beads coated with an anti-JAM-A mAb, although able to effectively adhere on the cell surface, were unable to induce integrin clustering (Fig. 7). Taken together, these data suggest that clustering of β1 integrin recruits JAM-A, which might then be co-internalized in the same intracellular compartments.

We then asked whether integrin internalization requires JAM-A. To this aim, we isolated neutrophils from JAM-A-null mice. As reported in Fig. 8, similarly to human cells, JAM-A was mostly concentrated in intracellular vesicles in mouse neutrophils. Such vesicles became more abundant following stimulation with the chemotactic peptide WKYMVm, which has a higher affinity for the mouse fMLP receptor (He et al., 2000). As expected, JAM-A-null neutrophils did not show detectable staining with the JAM-A antibody.

In JAM-A-positive cells, β1 integrins were concentrated at the cell surface and in intracellular vesicles similarly to their distribution in human neutrophils. By contrast, confocal analysis of JAM-A$^{+/+}$ and JAM-A$^{-/-}$ neutrophils surface-labeled with an anti-integrin-β1 antibody at 4°C and then incubated at 37°C with or without WKYMVm, revealed that in JAM-A-null neutrophils, β1 integrins displayed a strongly altered distribution, being present in numerous small cell-surface clusters rather than diffuse on the cell surface (Fig. 9A).

Western blotting (supplementary material Fig. S6, using MB1.2 mAb) and FACS analysis (using mAb 9Eg7) (data not shown) showed that the amount of total and activated β1 integrin was unchanged in the presence or absence of JAM-A, suggesting that this protein does not directly modify integrin expression and activation in cells in suspension.

To investigate the role of JAM-A in regulating integrin turnover, neutrophils derived from JAM-A WT and knockout mice were subjected to an immunofluorescence-based recycling assay (see Materials and Methods) (Jovic et al., 2007), to compare the levels of internalized β1 integrin in polarized JAM-A$^{+/+}$ and JAM-A$^{-/-}$ neutrophils. The cells were surface-labeled by the incubation of living cells with the anti-β1 integrin antibody at 4°C. Cells were then allowed to migrate for 15 minutes at 37°C, upon chemotactic stimulation. Under these conditions, the integrin-antibody complexes could internalize and in part recycle to the plasma membrane in response to chemokine stimulation. The complexes recycled to the membrane were stripped off with an acid wash, while

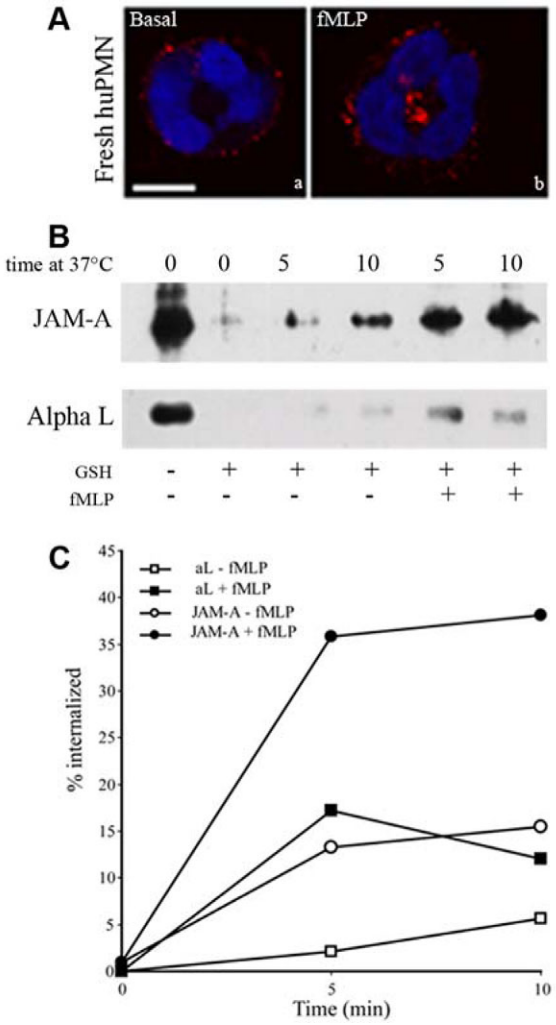

Fig. 4. JAM-A is internalized in neutrophils upon fMLP treatment. (A) Immunofluorescence internalization analysis of JAM-A endocytosis from the plasma membrane in fresh human neutrophils, either treated (b) or not (a) with fMLP. JAM-A internalized vesicles (red) are more abundant in activated cells. Each panel is a single projection of a *z*-stack of three confocal sections (stack *z*-spacing, 0.3 μm). Cell nuclei were counterstained with DAPI (blue). Scale bars: 5 μm. (B) Freshly purified neutrophils were labeled at 4°C with cleavable biotin and left untreated or stimulated with fMLP for 5 and 10 minutes at 37°C before surface biotin cleavage with GSH, and lysis. Biotinylated proteins were precipitated with streptavidin-agarose followed by western blot analysis with anti-JAM-A (BV22 mAb) and anti-αL integrin (clone 27) antibodies. (C) Densitometric analysis of internalized JAM-A and αL integrin normalized for their total amount. The figure shows one representative experiment out of five performed.

the internalized β1 integrin-antibody complexes were detected with secondary antibodies under permeabilizing conditions by confocal analysis. As shown in Fig. 9B, the amount of internalized β1 integrin in JAM-A$^{-/-}$ neutrophils was significantly reduced compared with JAM-A$^{+/+}$ cells, whereas β1 integrin present on the cell surface was markedly increased (Fig. 9A).

We also quantified the difference between JAM-A$^{+/+}$ and JAM-A$^{-/-}$ neutrophils in the amount of integrin expressed on the cell surface by FACS analysis. JAM-A$^{+/+}$ and JAM-A$^{-/-}$ neutrophils treated before fixation with the anti-integrin-β1 antibody were stimulated with the chemotactic peptide, trypsinized and analyzed with secondary antibody by FACS analysis. As reported in Fig. 9C, in the absence of JAM-A and before acid wash, surface integrin β1 levels were 50% higher than in JAM-A-positive neutrophils, as shown by immunofluorescence analysis (Fig. 9A). The acid wash fully eliminated surface antibody staining in both conditions. Moreover, FACS analysis of living cells treated with the anti-integrin antibody, acid washed and further incubated at 37°C with the chemotactic peptide to allow surface integrin recycling, revealed that the recycling of integrins to the cell surface upon internalization was 50% lower in JAM-A-null neutrophils (Fig. 9C).

Finally, we tested whether integrin internalization in JAM-A$^{-/-}$ neutrophils was also impaired in vivo. Distribution of β1 integrins in neutrophils was analyzed in the mouse cremaster muscle after 4 hours of stimulation with LTB4 using immunostaining and confocal deconvolution microscopy. A significantly smaller amount of internalized integrins was observed in neutrophils from mutant mice compared with control mice (Fig. 9D). Overall, these data support the hypothesis that JAM-A is required for optimal internalization and recycling of integrins in neutrophils activated by chemotactic stimuli.

If this was the case, the phenotype of JAM-A-null neutrophils, characterized by an elongated uropod as well as by defective cell polarization and directional migration, might be due to a defect in integrin detachment from the substratum and recycling along the direction of movement (Caswell and Norman, 2006; Jones et al., 2006; Lawson and Maxfield, 1995; Pierini et al., 2000). To prove this possibility, we treated both JAM-A$^{+/+}$ and JAM-A$^{-/-}$ neutrophils with BAPTA-AM, a known inhibitor of integrin recycling (Hellberg et al., 1995; Rowin et al., 1998). Upon BAPTA-AM treatment, the uropod of JAM-A$^{+/+}$ cells was strongly elongated in a way comparable to that in JAM-A$^{-/-}$ cells (Fig. 10). Conversely, BAPTA-AM treatment did not further modify this morphological feature in JAM-A-null cells. Altogether, these data support the idea that JAM-A promotes leukocyte directional migration by controlling the integrin endo-exocytic cycle.

The mechanism of action of JAM-A in inhibiting integrin internalization remains to be fully characterized. The small GTPase Rap-1 governs integrin functions and integrin-mediated phagocytosis (for a review, see Cougoule et al., 2004). In epithelial cells, JAM-A colocalizes with Rap-1 and is required for its activation (Mandell et al., 2005). Therefore, we tested whether JAM-A can also influence Rap-1 activity in neutrophils. We found that Rap-1 activation was detectable in resting mouse neutrophils and did not increase further upon WKYMVm activation possibly because it is extremely difficult to fully prevent activation of these cells during separation. In the absence of JAM-A, Rap-1 activity was barely detectable in either resting or activated conditions (Fig. 11).

These data suggest that JAM-A, similarly to other cell types, might regulate integrin activity and internalization by modulating Rap-1 activity.

Discussion

Despite its reported activity in several in vivo models of inflammation, the mechanism of action of JAM-A remains elusive. Its absence, or inhibition with blocking antibodies, prevents neutrophil emigration from the vessel wall. This effect has been ascribed to the junctional localization of JAM-A in the vascular endothelium, which might be required to direct neutrophil transmigration through the endothelial cleft (Bazzoni and Dejana, 2004; Bradfield et al., 2007; Vestweber, 2007; Weber et al., 2007). However, we observed previously that JAM-A expressed on

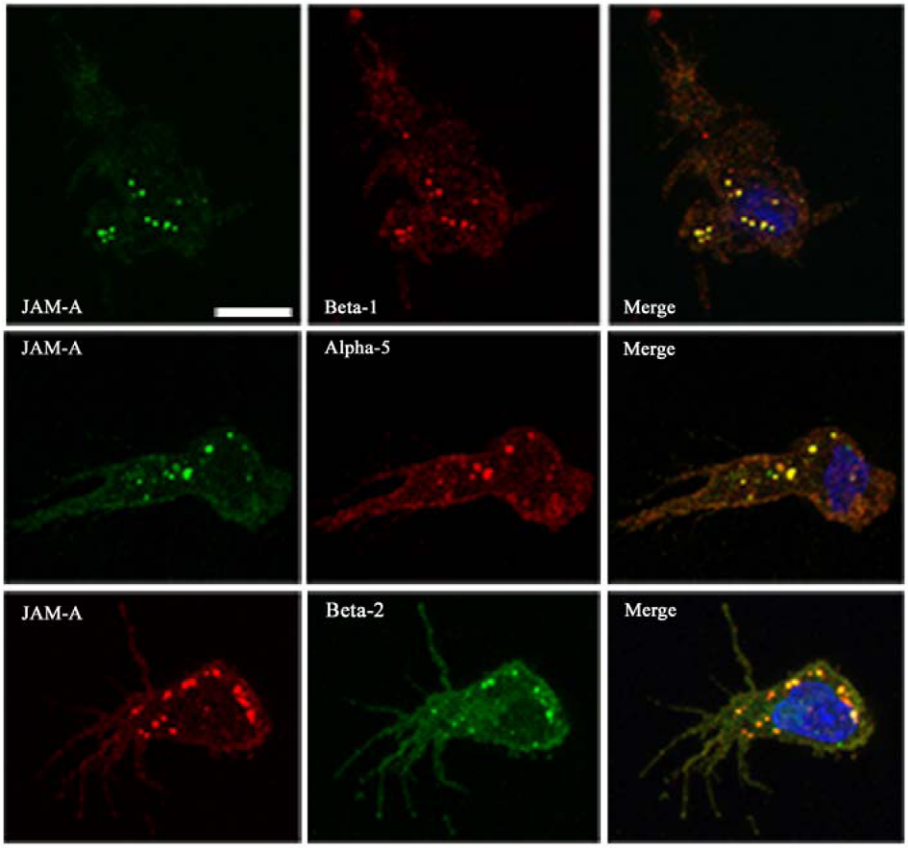

Fig. 5. JAM-A colocalizes with α5β1 and β2 integrins. Double staining of JAM-A (green) and α5β1 integrins (red) or JAM-A (red) and β2 integrin (green) in polarized dHL60 cells. The cells were seeded on fibronectin-coated coverslips, treated with fMLP for 20 minutes and incubated with anti-JAM-A and anti-β1 integrin antibodies before paraformaldehyde fixation. Each panel represents a single projection of a *z*-stack of about three confocal section (stack *z*-spacing, 0.4 μm). Merged images show JAM-A colocalization with integrins. Cell nuclei are counterstained with DAPI (blue). Scale bar: 5 μm. The figure shows one representative experiment out of five performed.

neutrophils could positively influence their directional migration in vitro (Corada et al., 2005). Here, we report for the first time in vivo that, after extravasation, neutrophil migration within the interstitial tissue is significantly impaired in JAM-A-deficient mice. Under these inflammatory conditions, JAM-A deficiency had no effect on previous steps of the leukocyte recruitment process, including rolling, firm adherence and transmigration (Woodfin et al., 2007). These data confirm the cell autonomous role of JAM-A on neutrophil chemotaxis in an in vivo system.

In the effort to investigate the mechanism of action of JAM-A, we found that this molecule might interact with neutrophil β1 integrins and positively modulate their internalization and recycling. Several lines of evidence support this conclusion. First, upon activation with chemotactic stimuli, HL60 cells or freshly isolated neutrophils can promptly internalize JAM-A in intracellular vesicles where it codistributes with β1 integrins. Second, β1 integrin clustering induced by beads coated with fibronectin or anti-integrin antibodies induced co-clustering of JAM-A, supporting the concept that the two molecules interact in living cells. Third, and most importantly, the integrin endo-exocytic cycle, induced by chemotactic stimuli, is strongly inhibited in JAM-A-null neutrophils. In this paper, we mostly focused on β1 integrin, but β2 integrins also codistribute with JAM-A in intracellular vesicles, suggesting a general role for JAM-A on different types of integrins.

In our previous work, we observed that in the absence of JAM-A, neutrophils adhere more effectively to different substrata and, when activated by chemotactic stimuli, present elongated tails as a result of their frustrated effort to move and detach the uropod from the substratum (Corada et al., 2005). We propose that the lack of dynamic internalization of integrins in the absence of JAM-A is the cause of the strong and deregulated adhesion of neutrophils to the integrin substrata. Consistently with this hypothesis, we observed a comparable phenotype, with neutrophils displaying long uropods, after treating the cells with BAPTA-AM. By chelating intracellular Ca^{2+}, this agent was previously reported to prevent integrin recycling

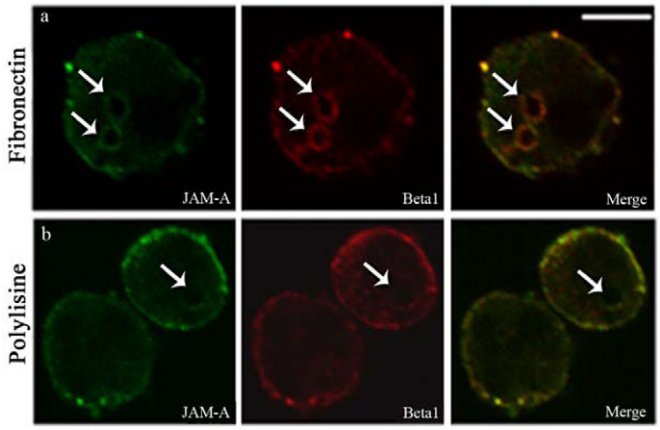

Fig. 6. Fibronectin-induced co-clustering of JAM-A with integrins. Immunofluorescence staining of dHL60 cells incubated with either fibronectin-coated or polylysine-coated beads. After incubation with the beads, cells were fixed and double stained with antibodies against JAM-A and integrin β1. (a) JAM-A and β1 integrin co-clustering at the bead contact sites (arrows); (b) Polylysine-coated beads do not induce co-clustering (arrows). Single projections of *z*-stacks of two confocal sections (stack *z*-spacing, 0.3 μm) are shown. Scale bar: 5 μm. The figure shows one representative experiment out of four performed.

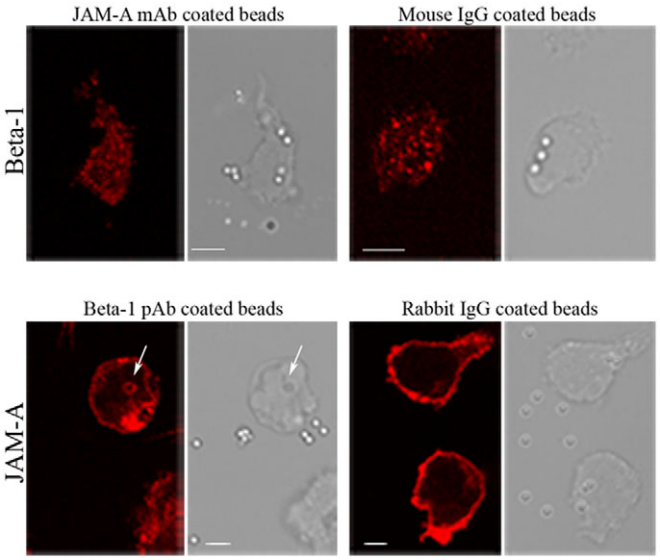

Fig. 7. Integrins induce JAM-A clustering. Immunofluorescence staining of dHL60 cells incubated with beads coated with JAM-A mAb (BV16) or a β1 integrin pAb, mouse or rabbit IgGs respectively. Cells were fixed and stained as in Fig. 6. β1-integrin-pAb-coated beads induced JAM-A clustering (arrows), whereas JAM-A-mAb-coated beads were unable to recruit integrin β1. Beads coated with either mouse or rabbit IgGs were not effective. Single projections of *z*-stacks of about two confocal sections (stack *z*-spacing, 0.3 μm) are shown. Scale bars: 5 μm. The figure shows one representative experiment out of two performed.

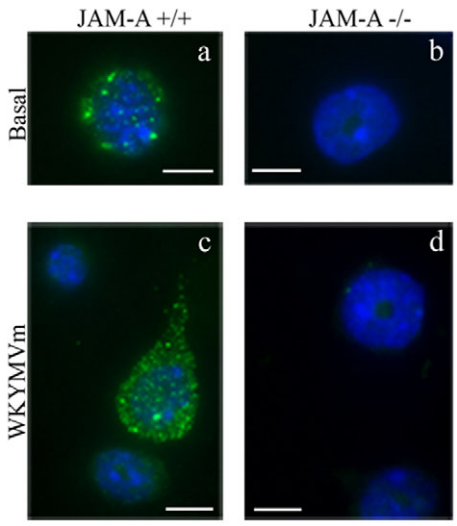

Fig. 8. JAM-A concentrates in intracellular vesicles in murine neutrophils. Immunofluorescence analysis of neutrophils derived from bone marrow of JAM-A$^{+/+}$ and JAM-A$^{-/-}$ mice. Living cells were treated with an anti-murine JAM-A mAb (BV12) and then seeded on fibronectin-coated coverslips and fixed. Untreated (a,b) or WKYMVm-activated (c,d) cells are shown. The nuclei of the cells are counterstained with DAPI (blue). Murine neutrophils show JAM-A localization at intracellular vesicles, whereas, as expected, JAM-A was undetectable in JAM-A$^{-/-}$ cells (b,d). Scale bars: 5 μm. The figure shows one representative experiment out of four performed.

to the cell surface and to abrogate directed migration induced by chemotactic gradients (Rowin et al., 1998).

The direct or indirect interaction of JAM-A with different types of integrins and in different cell types has been previously described. In endothelial cells, it was found that JAM-A directly binds αvβ3 integrins and that this association promotes cell migration (Naik et al., 2003; Naik and Naik, 2006). Furthermore, in epithelial cells, JAM-A controls integrin β1 internalization and degradation (Mandell et al., 2005). It has also been reported that JAM-A expressed in endothelial cells might interact with αLβ2 integrins on leukocytes and that this interaction mediates adhesion and transmigration of these cells (Ostermann et al., 2005; Ostermann et al., 2002).

A still unexplained aspect of the physiological role of JAM-A is that it appears to exert different and in some cases even opposite effects in different cell types. For instance, the absence of JAM-A increases dendritic cell motility to lymph nodes (Cera et al., 2004). Similarly, JAM-A-null endothelial or epithelial cells show increased random motility (Bazzoni et al., 2005; Mandell et al., 2005). It is possible that the activity of JAM-A varies depending on the type of integrin expressed by the different cell types. Furthermore, JAM-A might also act through other mechanisms, such as tubulin organization (Bazzoni et al., 2005), which might affect the migratory phenotype of selected cell types, such as the endothelium, compared with others, such as neutrophils. In support of this, in preliminary work we did not see any difference in tubulin organization and microtubule-organizing center (MTOC) localization in JAM-A-null neutrophils compared with wild-type cells (M.R.C., unpublished observations), whereas significant changes were observed in endothelial cells lacking JAM-A (Bazzoni et al., 2005).

Small GTPases are implicated in integrin internalization and recycling. Elongated tails and reduced transendothelial migration were found in cells treated with Rho inhibitors (Worthylake et al., 2001), and in general, Rac and Rho GTPases are important for orchestrating polarized cell migration (for reviews, see Jaffe and Hall, 2005; Ridley et al., 2003). In preliminary work, we did not find evidence of Rho or Rac activation changes in JAM-A-knockdown assays. However, previous work showed that JAM-A and Rap-1 can codistribute in cultured epithelial cells at intercellular junctions and the knockdown of JAM-A resulted in decrease of Rap-1 activity (Mandell et al., 2005). Consistently, in the present paper we show that activation of Rap-1 is strongly reduced in JAM-A-null neutrophils. However, in contrast to epithelial cells, the knockdown of JAM-A reduced cell motility.

A likely explanation of this discrepancy is that in epithelial cells, in absence of JAM-A, β1 integrins are internalized and degraded, whereas in JAM-A-null neutrophils, expression or activation of β1 integrins do not significantly change, and integrins are instead recycled to the cell surface and contribute to cell motility (Hellberg et al., 1995; Rowin et al., 1998). Another important difference is that in epithelial cells, JAM-A and integrins are mostly localized to intercellular junctions, and knockdown of JAM-A increases cell motility by disrupting cell-cell contacts (Mandell et al., 2005). Unlike cells in the epithelium, leukocytes do not form intercellular junctions; it is therefore conceivable that in these cells, JAM-A modulation of integrin activity results in different downstream effects.

In a recent paper, Lammermann et al. show that integrins are not required for leukocyte migration in a three-dimensional environment (Lammermann et al., 2008). We show here that without JAM-A, integrins are retained at the cell surface and their dynamic recycling

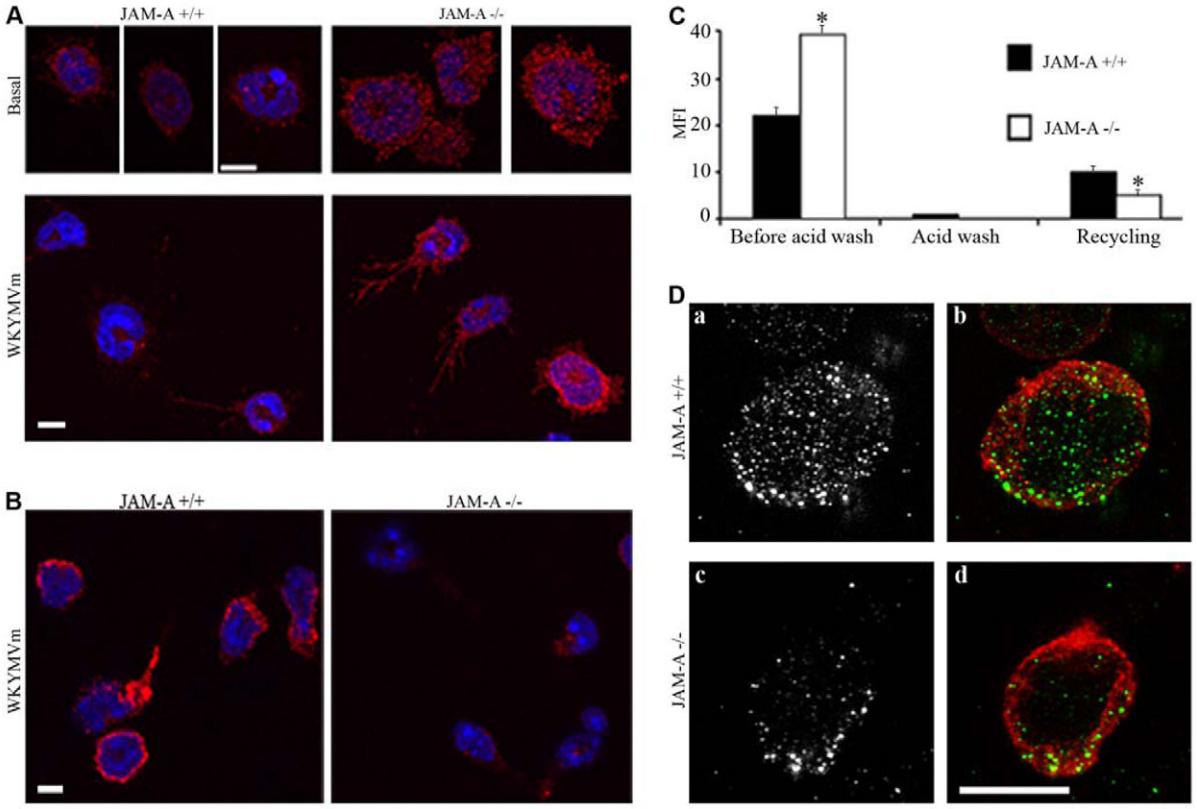

Fig. 9. Integrin internalization is altered in JAM-A$^{-/-}$ neutrophils. (A) Confocal immunofluorescence analysis of integrin β1 in mouse JAM-A$^{+/+}$ and JAM-A$^{-/-}$ neutrophils. Cells were seeded on fibronectin-coated coverslips, stimulated or not with the chemotactic peptide WKYMVm, fixed and stained. The images are single projections of *z*-stacks of about four confocal sections (stack *z*-spacing, 0.3 μm). Note the higher expression of β1 integrins at the plasma membrane of JAM-A$^{-/-}$ than JAM-A$^{+/+}$ neutrophils. Cell nuclei are counterstained with DAPI (blue). Scale bars: 5 μm. (B) Immunofluorescence internalization assay of integrin in JAM-A$^{+/+}$ and JAM-A$^{-/-}$ neutrophils. Cells were seeded on fibronectin-coated coverslips, treated with WKYMVm and then surface-labeled with the anti-integrin-β1 antibody. Cells were then incubated at 37°C to allow integrin internalization. The integrin-antibody complexes at the plasma membrane were removed by acid washing, whereas the internalized complexes were detected by confocal microscopy under permeabilizing conditions. Single projections of *z*-stacks of about five confocal sections (stack *z*-spacing, 0.3 μm) are shown. The amount of internalized integrin is reduced in JAM-A$^{-/-}$ compared with JAM-A$^{+/+}$ neutrophils. Cell nuclei are counterstained with DAPI (blue). Scale bar: 5 μm. (C) FACS recycling assay was used to quantify integrin recycling to the cell surface after internalization. The amount of integrin on the cell surface before acid wash was higher in JAM-A$^{-/-}$ neutrophils (white bars) compared with JAM-A$^{+/+}$ neutrophils (black bars). Acid washing abrogated surface staining in both cell types. The amount of integrin recycled to the cell surface after acid wash was higher in the presence than in the absence of JAM-A. MFI, mean fluorescence intensity. Data are means ± s.e.m. of triplicates from one representative experiment out of three performed. *P<0.05, by Student's *t*-test. (D) Distribution of β1 integrins in neutrophils was analyzed in the mouse cremaster muscle after 4 hours of stimulation with LTB4 using immunostaining and confocal deconvolution microscopy. Representative confocal microscopic images of β_1 integrin (green) localization in transmigrated neutrophils in the cremaster muscle of JAM-A$^{+/+}$ (a,b) and JAM-A$^{-/-}$ mice (c,d). A projection of *z*-planes covering 2.5 μm is shown (projection of ten *z*-planes; *z*-spacing, 250 nm). Comparative membrane staining was done using a CD45 antibody (red). A significantly smaller amount of internalized integrins was observed in neutrophils of JAM-A$^{-/-}$ mice. Scale bar: 5 μm.

is impaired. This suggests that, in JAM-A-null leukocytes, integrins might act as immobilizing anchors that slow down cell motility, both by increasing adhesion and possibly by changing the overall dynamics of the cytoskeleton, inhibiting cell squeezing in a 3D matrix.

In conclusion, here we provide evidence that JAM-A influences neutrophil motility in a cell-autonomous manner, through modulation of integrin internalization and recycling. When this activity is impaired, as in JAM-A-null mice, the response to inflammatory reactions and ischemia reperfusion injury is strongly affected.

Materials and Methods

Cells and flow cytometry

HL-60 promyelocytic leukemia cells were obtained from the American Type Culture Collection (ATCC, Manassas, VA) and cultured as described (Newburger et al., 1979). Differentiated HL60 (dHL60) cells were obtained by treating 2×10^5 cells per ml with complete medium supplemented with 1.25% dimethyl sulfoxide (DMSO, Sigma) for 5 days. All the tissue culture reagents were purchased from Life Technologies, Paisley, UK. Human neutrophils were isolated from fresh heparinized blood (50 ml) of healthy human volunteers by dextran sedimentation, followed by Ficoll-Hypaque gradient centrifugation as previously described (Fabbri et al., 2005). Mouse bone marrow neutrophils were purified (90-95% purity) as previously described (Lowell et al., 1996). Fluorescence flow cytometric analysis was performed by a FACStar Plus apparatus (Becton Dickinson) as previously described (Balconi et al., 2000). JAM-A expression was analyzed using the mouse anti-human JAM-A BV16 mAb produced in our laboratory (Williams et al., 1999), and a FITC-conjugated donkey anti-mouse (Jackson Immuno Research Laboratories) as secondary antibody.

Immunoprecipitation and western blot

HL60 cells were washed with ice-cold PBS and extracted on ice in lysis buffer (50 mM Tris-HCl, pH 7.4, 150 mM NaCl, 1% Triton X-100, 10% glycerol), supplemented with a cocktail of protease inhibitors (Set III; Calbiochem). The pre-cleared cell lysates were immunoprecipitated overnight at 4°C with the anti-human JAM-A BV16 antibody-bound G-agarose beads (Amersham) or with the anti-human integrin β1 antibody (clone B44, Chemicon). For the integrin β2 immunoprecipitation, pre-chilled cells were surface biotinylated by incubation with 1 mg/ml EZ-Link sulfo-NHS-LC-Biotin (Pierce) for 1 hour on ice. Cells were washed three times in PBS with 10 mM glycine before immunoprecipitation. The anti-human integrin β2 Ts1/18 and anti-

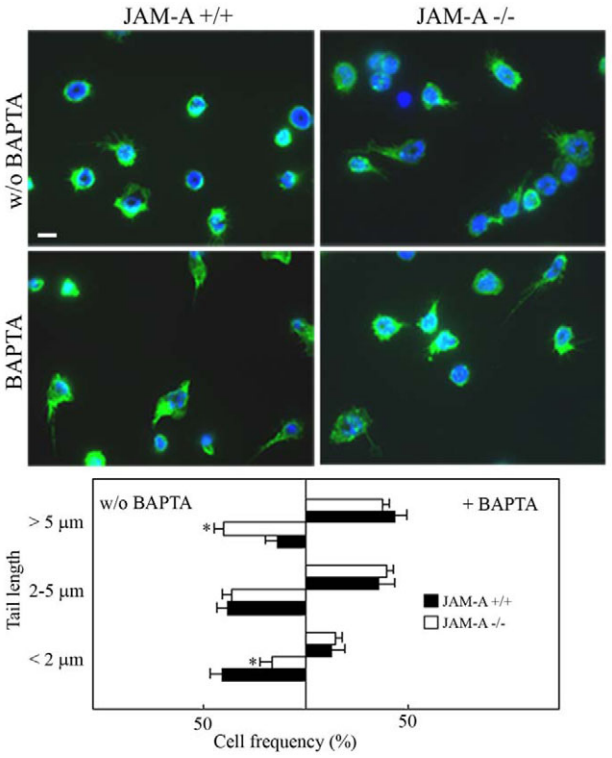

Fig. 10. BAPTA-AM treatment alters the uropod length of JAM-A$^{+/+}$ neutrophils. Actin immunofluorescence staining of JAM-A$^{-/-}$ and $^{+/+}$ murine neutrophils is shown. To block integrin internalization, cells were pre-incubated with BAPTA-AM where indicated. The number of cells showing long tails was increased upon BAPTA-AM treatment of JAM-A$^{+/+}$ cells, whereas uropod lengths were not altered in JAM-A$^{-/-}$ neutrophils. Cell nuclei are counterstained with DAPI (blue). Scale bar: 5 µm. The length of neutrophil tails was measured using Carnoy software version 2.0 for Macintosh and the frequency of cells with different tail size is reported for the two populations (JAM-A$^{+/+}$, black columns; JAM-A$^{-/-}$, white columns). The graph shows the means ± s.e.m. of four experiments. *P<0.01, Student's t-test.

human integrin αL Ts1/22 (kind gifts of Ruggero Pardi, Dibit-Scientific Institute San Raffaele, Milan, Italy) were used for immunoprecipitation.

For western blot, analysis the mouse anti-human JAM-A BV22 mAb (produced in our laboratory) (Williams et al., 1999), the rat anti-mouse β1 integrin (clone MB1.2, Chemicon) and the mouse anti-human αL integrin mAb (clone 27, BD-Pharmingen) were used.

Internalization assay

Internalization was evaluated as described previously (Fabbri et al., 2005). Freshly purified human neutrophils (5×10^6) or dHL60 cells (10^7) were cooled on ice and washed in pre-chilled PBS before incubation with PBS 0.5 mg/ml thiol-cleavable Sulfo-NHS-S-S-Biotin (Pierce Chemical Co.) for 1 hour on ice. After washing with ice-cold PBS, labeled cells were resuspended in serum-free RPMI medium supplemented or not with 100 nM fMLP (Sigma) and incubated for the indicated time points at 37°C to allow internalization. Samples were then returned to ice, washed three times with ice-cold PBS, and treated with two successive reductions of 20 minutes with a reducing solution containing the non-membrane permeable reducing agent glutathione (GSH; 42 mM), 75 mM NaCl, 1 mM EDTA, 1% bovine serum albumin and 75 mM NaOH. To evaluate total labeling, a sample was not reduced with GSH. To control background, a sample was labeled and reduced without incubation at 37°C. Cells were then washed and lysed in 500 µl of a solution containing 10 mM Tris-HCl (pH 7.6), 150 mM NaCl, 1 mM $CaCl_2$, 1 mM $MgCl_2$, and 1% NP-40 on ice. Biotinylated proteins were then precipitated with streptavidin-agarose (GE Healthcare). Samples were analyzed by SDS-PAGE, transferred onto nitrocellulose, and revealed with anti-JAM-A and anti-integrin αL (clone 27, BD Biosciences, San José, CA).

Cell immunofluorescence microscopy

dHL60 cells (2×10^5) were washed with RPMI 0.1% BSA and seeded on fibronectin-coated (20 µg/ml) coverslips (13 mm diameter). Cells were allowed to adhere for 10 minutes at 37°C and then were stimulated with fMLP (100 nM) or PMA (10 ng/ml; from Sigma) for 20 minutes at 37°C. dHL60 cells were stained either as living cells (primary antibody incubated with live cells; see Immunofluorescence internalization assay methods) or after cell fixation (primary antibody after fixation) as previously described (Pierini et al., 2000). In both cases, cells were fixed with 3.7% paraformaldehyde (paraformaldehyde) for 15 minutes at room temperature. Blocking was performed in PBS containing 10% FBS and 2 mg/ml BSA (Blocking solution) for 1 hour at room temperature, and then for 30 minutes in PBS containing 5% serum specific to the species of the secondary antibody. Then, cells were permeabilized with PBS containing 0.5 mg/ml saponin for 10 minutes at room temperature. Saponin was maintained for the entire staining procedure. Labeling with primary antibodies or appropriate fluorescent-conjugated secondary antibodies (Jackson ImmunoResearch) was performed in Blocking solution supplemented with 0.25 mg/ml saponin for 1 hour at room temperature.

JAM-A staining after fixation of fMLP-treated dHL60 cells was obtained with the rabbit anti-human JAM-A pAb (Zymed) in cells fixed with ice-cold methanol (5 minutes on ice). For α5 integrin staining, cells were fixed and permeabilized simultaneously by incubation with 6.6% paraformaldehyde/0.05% glutaraldehyde/0.25 mg/ml saponin in PBS for 5 minutes at 37°C (Pierini et al., 2000). For JAM-A staining, bone-marrow-purified murine neutrophils (0.4×10^6 cells) were seeded in RPMI, 0.1% BSA on fibronectin-coated (10 µg/ml) coverslips (13 mm diameter) for 20 minutes at 37°C. Following pre-chilling on ice for 20 minutes, living cells were treated with the anti-JAM-A mAbs (BV12 or BV20, produced in our laboratory (Martin-Padura et al., 1998), in RPMI, 0.1% BSA for 30 minutes at 4°C (2 µg/sample). Cells were washed with pre-chilled RPMI and then incubated with 5 nM WKYMVm (a kind gift from Giorgio Berton and Laura Fumagalli, University of Verona, Verona, Italy) in RPMI, 0.1% BSA for 15 minutes at 37°C. Cells were then fixed with 3.7% paraformaldehyde for 15 minutes at room temperature and permeabilized with PBS containing 0.1% Triton X-100 for 5 minutes at 4°C. Blocking and immunofluorescence staining was performed as described above.

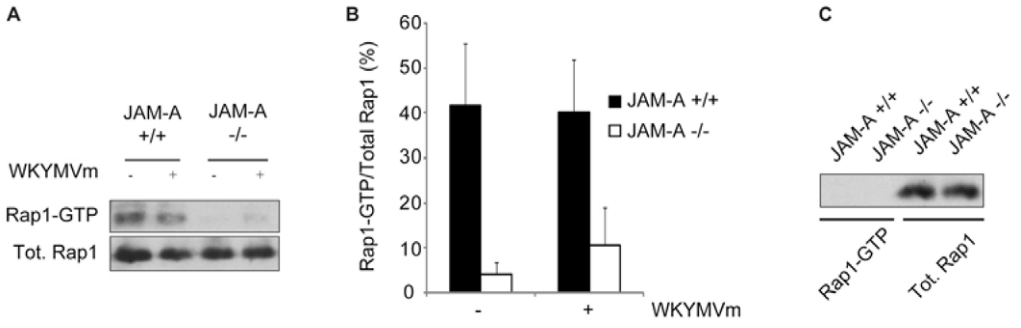

Fig. 11. Rap-1 activation is impaired in JAM-A$^{-/-}$ neutrophils. A pull-down assay was performed to isolate active GTP-bound Rap-1. Freshly isolated mouse neutrophils were obtained from JAM-A$^{+/+}$ and JAM-A$^{-/-}$ mice. 5×10^6 cells for each condition were left untreated or stimulated with the chemotactic peptide WKYMVm for 5 minutes at 37°C. Pull down was performed on cell lysates using the RalGDS-RBD probe (A) or the GST-negative control (C). Western blot for Rap-1 revealed impaired Rap-1 activation in both unstimulated and stimulated JAM-A$^{-/-}$ compared with JAM-A$^{+/+}$ neutrophils. (B) Densitometric analysis of active GTP-bound Rap-1 normalized for the total amount of protein. Results in B are means ± s.e.m. of four separate experiments; A and C show a typical experiment.

For actin distribution or β1 integrin staining, bone-marrow-purified neutrophils (0.4×10^6 cells) were seeded on fibronectin-coated (20 μg/ml in PBS) coverslips for 10 minutes at 37°C, before incubation with 5 nM WKYMVm for 20 minutes at 37°C. Cells were then fixed with 3.7% paraformaldehyde for 20 minutes at room temperature and permeabilized with PBS 0.1% Triton X-100 for 5 minutes (room temperature).

In some experiments, before seeding on fibronectin-coated coverslips, bone-marrow-purified murine neutrophils were incubated at 37°C for 30 minutes in HBSS medium without Ca^{2+}/Mg^{2+} supplemented with 0.1% BSA, 1 mM EGTA and 50 μM BAPTA-AM [1,2-bis (o-Aminophenoxy) ethane-N,N,N′,N′-tetraacetic acid tetra (acetoxymethyl) ester] (Calbiochem). Before mounting, cell nuclei were stained with 4′,6-diamidino-2-phenylindole (DAPI; Jackson ImmunoResearch) for 5 minutes at room temperature. Coverslips were then mounted in Mowiol 4-88 (Calbiochem-Novabiochem, La Jolla, CA).

Primary antibodies used in immunofluorescence microscopy were: rat anti-mouse JAM-A mAbs BV12, BV20, mouse anti-human α5 integrin (CD49e) biotin-conjugated (clone VC5, BD-Pharmingen), mouse anti-human CD18 FITC-conjugated (clone MEM 48, Chemicon), mouse anti-human JAM-A BV16, BV17, BV22 (antibodies produced in our laboratory) (Williams et al., 1999) and mouse anti-human VE-cadherin TEA (produced in our laboratory) (Corada et al., 1999). Actin staining was performed using Alexa Fluor 546- or 488-labeled phalloidin (Molecular Probes). In experiments with living cells, BV16, BV22, BV12 and BV20 were used as purified immunoglobulin G (IgG). Purified non-immune rat IgG (Jackson ImmunoResearch, West Grove, PA) were used as controls.

In double-labeling experiments, $F(ab')_2$ fluorophore-labeled secondary antibodies with minimal cross-reactivity to other species, except for the targeted ones, were used (Jackson Immuno Research Laboratories). After incubation with the secondary antibody to the first antigen, cells were further fixed with paraformaldehyde (5 minutes, room temperature) before labeling with the second antigen.

All slides were analyzed with a fluorescence microscope (Leica DMR, Wetzlar, Germany). Images were recorded with a Hamamatsu 3CCD camera (Hamamatsu Photonics, Hamamatsu City, Japan). Where specified, a Leica TCS SP2 AOBS filter-free spectral confocal microscope and its dedicated Leica Confocal Software (Leica Microsystems, Mannheim, Germany) were used. Images were processed using ImageJ 1.30k, freely available at http://rsb.info.nih.gov/ij/java1.3.1/, and Adobe Photoshop 8.0 (Adobe Systems, San Jose, CA).

Immunofluorescence internalization assay

dHL60 cells were treated as living cells with the anti-JAM-A BV16 mAb and acid washed before fixation (Lampugnani et al., 2006; Lawson and Maxfield, 1995). Cells were washed in RPMI, 0.1% BSA and pre-cooled on ice before treatment with 15 μg/ml antibody (2×10^5 cells in 100 μl RPMI, 0.1% BSA with mAb) for 30 minutes on ice with gentle agitation. After washing with ice-cold RPMI, 0.1% BSA to remove unbound antibody, cells were seeded on fibronectin-coated coverslips and stimulated with 100 nM fMLP for 20 minutes at 37°C. Before fixation, cells were placed on ice and acid washed (three washes with ice-cold 50 mM glycine in Ca^{2+}/Mg^{2+} HBSS, pH 2.5, and two washes with Ca^{2+}/Mg^{2+} HBSS, pH 7.5) to remove the antibody from the cell surface. Cells were then fixed, permeabilized, and stained as described above.

Immunofluorescence recycling assay and FACS recycling assay

The immunofluorescence recycling assay was performed as previously described (Jovic et al., 2007), with minor modifications. Mouse bone-marrow-derived neutrophils (2×10^5 cells) were seeded in RPMI 0.5% BSA on fibronectin-coated (20 μg/ml) coverslips (13 mm diameter) for 10 minutes (37°C) before incubation with 5 nM WKYMVm for 20 minutes (37°C). Then, cells were pre-cooled on ice for 20 minutes and incubated with the rat anti-integrin β1 mAb (clone 9Eg7; BD-Pharmingen) for 30 minutes at 4°C. Cells were washed with ice-cold RPMI 0.5% BSA to remove unbound antibody before further incubation with 5 nM WKYMVm for 15 minutes at 37°C. Before fixation, cells were placed on ice and washed or not with an acid buffer (see immunofluorescence internalization assay methods) to remove the integrin-antibody complexes from the cell surface. Cells were fixed with 3.7% paraformaldehyde for 15 minutes at room temperature and permeabilized with PBS 0.1%, Triton X-100 for 5 minutes (room temperature). Staining with secondary antibody was performed as previously described.

To quantify β1 integrin recycling by flow cytometry, mouse bone-marrow-derived neutrophils were treated as indicated above with the exception that after the acid stripping the cells were further incubated with 5 nM WKYMVm for 20 minutes at 37°C. Following trypsinization and pelleting, cells were incubated under non-permeabilizing conditions with FITC-conjugated goat anti-rat secondary antibody (Jackson Immuno Research Laboratories) for 30 minutes, and fixed in 4% paraformaldehyde in PBS.

Bead-binding assay

The bead-binding assay was performed as previously described (Tran et al., 2002). Polystyrene microbeads (1-3 μm diameter; Polysciences) were coated with 50 μg/ml fibronectin, 100 μg/ml polylysine (Sigma), 100 μg/ml mouse anti-human JAM-A BV16 or 100 μg/ml rabbit anti-β1 integrin (Chemicon) in 0.1 M Borate buffer (pH 8.5) at 4°C overnight. Purified non-immune rabbit and mouse IgG (Jackson ImmunoResearch) were used as controls. The ligand-coated beads were blocked with 1% BSA in PBS for 1 hour at room temperature. Glass coverslips (13 mm diameter) were coated with 20 μg/ml polylysine in PBS overnight at 4°C, and then blocked with 1% heat-denatured BSA for 1 hour at room temperature. Differentiated HL60 cells (2×10^5) were plated on polylysine-coated coverslips and stimulated with fMLP as previously described. In some experiments, living cells were treated with anti-JAM-A antibody (BV16 mAb). Ligand-coated beads were then added to the cells at a ratio of ten beads per cell and incubated for 20 minutes at 37°C. The cells were fixed with paraformaldehyde, and immunofluorescence analysis with mouse anti-human JAM-A BV16 and rat anti-integrin-β1 (clone 9Eg7) antibodies was performed according to the procedure described above. In some experiments, as controls, immunofluorescence analysis with the mouse anti-MHC class I mAb W632 antibody (a kind gift from Edgar Engleman, Stanford University, Palo Alto, CA) was performed.

Rap1 activation assay using RalGDS-RBD

Rap1 pull-down assays were performed using the GST-fused Rap1-binding domain of Ral GDS obtained by transforming *E. coli* strain BL21 with a pGEX-2T-RalGDS-RBD expression vector (Self et al., 2001). The fusion protein was affinity purified on Glutathione-Sepharose 4B beads (GE Healthcare) by standard methods. Rap1 pull-down assays were performed as described (Franke et al., 1997).

Rabbit polyclonal anti-Rap1 (Santa Cruz Biotechnology) and anti-rabbit HRP-conjugated (Cells Signaling Technology) antibodies were used to reveal Rap1-GTP and total Rap1. Densitometric analysis was performed using ImageJ imaging software.

In vivo experiments

Male C57BL/6J wild-type ($JAM\text{-}A^{+/+}$) mice were purchased from Charles River (Sulzfeld, Germany) and JAM-A-deficient mice ($JAM\text{-}A^{-/-}$) were generated as described previously (Cera et al., 2004). These mice have been previously backcrossed to a pure C57BL/6J genetic background. The surgical preparation of the mouse cremaster muscle was performed as originally described by Baez (Baez, 1973) and optical analysis was performed as described previously (Mempel et al., 2003). For off-line analysis of parameters describing the sequential steps of leukocyte extravasation, we used the Cap-Image image analysis software (Heinrich Zeintl, Heidelberg, Germany). Rolling and firm adherent leukocytes were defined as described previously (Ley et al., 1995). Transmigrated cells were counted in regions of interest (ROI), covering 75 μm on both sides of a vessel over 100 μm vessel length. For the analysis of leukocyte interstitial migration, ROIs were subdivided into a segment adjacent to the vessel covering 25×100 μm and a segment distant to the vessel covering 50×100 μm (Fig. 1A). Leukocyte accumulation in each segment was quantified and shown as a proportion of the number of transmigrated leukocytes in the total area.

After surgical preparation, one vessel segment was randomly chosen in a central area of the spread-out cremaster muscle of WT and $JAM\text{-}A^{-/-}$ mice among those vessel segments that were at least 150 μm away from neighboring postcapillary venules, and did not branch over a distance of at least 150 μm. After obtaining baseline recordings, leukocyte recruitment to the cremaster muscle was induced by topical application of leukotriene B4 (LTB4; 10^{-7} M; Calbiochem, La Jolla, CA). After 10, 20, 30, 40, 50 and 60 minutes, in vivo microscopic measurements were repeated (see above).

Data analysis was performed with a statistical software package (SigmaStat for Windows, Jandel Scientific, Erkrath, Germany). The Rank-Sum-Test was used for the estimation of stochastic probability in intergroup comparisons. Mean values and s.e.m. are given. Values of $P<0.05$ were considered significant. For the analysis of β1 integrin expression on transmigrated neutrophils in vivo, cremaster muscles were fixed in 4% paraformaldehyde. Tissues were then blocked and permeabilized in PBS, supplemented with 10% goat serum (Sigma) and 0.5% Triton X-100 (Sigma). After incubation at 4°C for 12 hours with the primary antibodies, a rabbit polyclonal anti-β1 integrin antibody (kindly donated by Ruggero Pardi) (Tomaselli et al., 1988) and a rat anti-mouse CD45 antibody (Ly-5, BD Pharmingen), tissues were incubated for 3 hours at room temperature with the secondary antibodies (Alexa Fluor 488-linked goat anti-rabbit and Alexa Fluor 568-linked goat anti-rat; Invitrogen). Immunostained tissues were mounted in PermaFluor (Beckman Coulter, Fullerton, CA) on glass slides and observed using a Leica SP5 confocal laser-scanning microscope (Leica Microsystems, Wetzlar, Germany) with an oil-immersion lens (Leica; ×63 NA 1.40). Z-stack digital images were collected optically at every 0.25 μm depth and deconvolved using the maximum likelihood estimation algorithm of Huygens Professional Deconvolution software (SVI, Hilversum, Netherlands). Further image processing was done using ImageJ software (National Institutes of Health, Bethesda, MD).

This work was supported by the Associazione Italiana per la Ricerca sul Cancro, Association for International Cancer Research, the European Community (Integrated Project Contract No LSHG-CT-2004-503573; NoE MAIN 502935; NoE EVGN 503254; EUSTROKE and OPTISTEM Integrated Projects), Istituto Superiore di Sanita', Italian Ministry of Health, MIUR (COFIN prot: 2006058482_002), Fondation

Leducq Transatlantic Network of Excellence, Deutsche Forschungsgemeinschaft (RE2885-1/1 to C.A.R.) and Friedrich-Baur-Stiftung (to M.R.) Data presented in this manuscript are part of the doctoral theses of M.R.C. and C.A.R.

References

Baez, S. (1973). An open cremaster muscle preparation for the study of blood vessels by in vivo microscopy. *Microvasc. Res.* **5**, 384-394.

Balconi, G., Spagnuolo, R. and Dejana, E. (2000). Development of endothelial cell lines from embryonic stem cells: a tool for studying genetically manipulated endothelial cells *in vitro*. *Arterioscler. Thromb. Vasc. Biol.* **20**, 1443-1451.

Bazzoni, G. and Dejana, E. (2004). Endothelial cell-to-cell junctions: molecular organization and role in vascular homeostasis. *Physiol. Rev.* **84**, 869-901.

Bazzoni, G., Tonetti, P., Manzi, L., Cera, M. R., Balconi, G. and Dejana, E. (2005). Expression of junctional adhesion molecule-A prevents spontaneous and random motility. *J. Cell Sci.* **118**, 623-632.

Bradfield, P. F., Nourshargh, S., Aurrand-Lions, M. and Imhof, B. A. (2007). JAM family and related proteins in leukocyte migration (Vestweber series). *Arterioscler. Thromb. Vasc. Biol.* **27**, 2104-2112.

Caswell, P. T. and Norman, J. C. (2006). Integrin trafficking and the control of cell migration. *Traffic* **7**, 14-21.

Cera, M. R., Del Prete, A., Vecchi, A., Corada, M., Padura, I. M., Motoike, T., Tonetti, P., Bazzoni, G., Vermi, W., Gentili, F. et al. (2004). Increased DC trafficking to lymph nodes and contact hypersensitivity in Junctional Adhesion Molecule-A-deficient mouse. *J. Clin. Invest.* **114**, 729-738.

Corada, M., Mariotti, M., Thurston, G., Smith, K., Kunkel, R., Brockhaus, M., Lampugnani, M. G., Martin-Padura, I., Stoppacciaro, A., Ruco, L. et al. (1999). Vascular endothelial-cadherin is an important determinant of microvascular integrity *in vivo*. *Proc. Natl. Acad. Sci. USA* **96**, 9815-9820.

Corada, M., Chimenti, S., Cera, M. R., Vinci, M., Salio, M., Fiordaliso, F., De Angelis, N., Villa, A., Bossi, M., Staszewsky, L. I. et al. (2005). Junctional adhesion molecule-A-deficient polymorphonuclear cells show reduced diapedesis in peritonitis and heart ischemia-reperfusion injury. *Proc. Natl. Acad. Sci. USA* **102**, 10634-10639.

Cougoule, C., Wiedemann, A., Lim, J. and Caron, E. (2004). Phagocytosis, an alternative model system for the study of cell adhesion. *Semin. Cell Dev. Biol.* **15**, 679-689.

Del Maschio, A., De Luigi, A., Martin-Padura, I., Brockhaus, M., Bartfai, T., Fruscella, P., Adorini, L., Martino, G. V., Furlan, R., De Simoni, M. G. et al. (1999). Leukocyte recruitment in the cerebrospinal fluid of mice with experimental meningitis is inhibited by an antibody to Junctional Adhesion Molecule (JAM). *J. Exp. Med.* **190**, 1351-1356.

Fabbri, M., Di Meglio, S., Gagliani, M. C., Consonni, E. R. M., Bender, J. R., Tacchetti, C. and Pardi, R. (2005). Dynamic partitioning into lipid rafts controls the endo-exocytic cycle of the aLb2integrin, LFA-1, during leukocyte chemotaxis. *Mol. Biol. Cell* **16**, 5793-5803.

Franke, B. J., Akkerman, J. W. and Bos, J. L. (1997). Rapid Ca^{2+}-mediated activation of Rap1 in human platelets.. *EMBO J.* **16**, 252-259.

He, R., Tan, L., Browning, D. D., Wang, J. M. and Ye, R. D. (2000). The synthetic peptide Trp-Lys-Tyr-Met-Val-D-Met is a potent chemotactic agonist for mouse formyl peptide receptor. *J. Immunol.* **165**, 4598-4605.

Hellberg, C., Eierman, D., Sjölander, A. and Andersson, T. (1995). The Ca^{2+} signaling capacity of the beta 2-integrin on HL60-granulocytic cells is abrogated following phosphorylation of its CD18-chain: relation to impaired protein tyrosine phosphorylation. *Exp. Cell Res.* **217**, 140-148.

Jaffe, A. B. and Hall, A. (2005). Rho GTPases: biochemistry and biology. *Annu. Rev. Cell Dev. Biol.* **21**, 247-269.

Jones, M. C., Caswell, P. T. and Norman, J. C. (2006). Endocytic recycling pathways: emerging regulators of cell migration. *Curr. Opin. Cell Biol.* **18**, 549-557.

Jonjic, N., Jilek, P., Bernasconi, S., Peri, G., Martin-Padura, I., Cenzuales, S., Dejana, E. and Mantovani, A. (1992). Molecules involved in the adhesion and cytotoxicity of activated monocytes on endothelial cells. *J. Immunol.* **148**, 2080-2083.

Jovic, M., Naslavsky, N., Rapaport, D., Horowitz, M. and Caplan, S. (2007). EHD1 regulates beta1 integrin endosomal transport: effects on focal adhesions, cell spreading and migration. *J. Cell Sci.* **120**, 802-814.

Khandoga, A., Kessler, J. S., Meissner, H., Hanschen, M., Corada, M., Motoike, T., Enders, G., Dejana, E. and Krombach, F. (2005). Junctional adhesion molecule-A deficiency increases hepatic ischemia-reperfusion injury despite reduction of neutrophil transendothelial migration. *Blood* **106**, 725-733.

Kornecki, E., Walkowiak, B., Naik, U. P. and Ehrlich, Y. H. (1990). Activation of human platelets by a stimulatory monoclonal antibody. *J. Biol. Chem.* **265**, 10042-10048.

Lammermann, T., Bader, B. L., Monkley, S. J., Worbs, T., Wedlich-Soldner, R., Hirsch, K., Keller, M., Forster, R., Critchley, D. R., Fassler, R. et al. (2008). Rapid leukocyte migration by integrin-independent flowing and squeezing. *Nature* **453**, 51-55.

Lampugnani, M. G., Orsenigo, F., Gagliani, M. C., Tacchetti, C. and Dejana, E. (2006). Vascular endothelial cadherin controls VEGFR-2 internalization and signaling from intracellular compartments. *J. Cell Biol.* **174**, 593-604.

Lawson, M. A. and Maxfield, F. R. (1995). Ca(2+)- and calcineurin-dependent recycling of an integrin to the front of migrating neutrophils. *Nature.* **377**, 75-79.

Ley, K., Bullard, D. C., Arbonés, M. L., Bosse, R., Vestweber, D., Tedder, T. F. and Beaudet, A. L. (1995). Sequential contribution of L- and P-selectin to leukocyte rolling *in vivo*. *J. Exp. Med.* **181**, 669-675.

Liu, Y., Nusrat, A., Schnell, F. J., Reaves, T. A., Walsh, S., Pochet, M. and Parkos, C. A. (2000). Human junction adhesion molecule regulates tight junction resealing in epithelia. *J. Cell Sci.* **113**, 2363-2374.

Lowell, C. A., Fumagalli, L. and Berton, G. (1996). Deficiency of Src family kinases p59/61hck and p58c-fgr results in defective adhesion-dependent neutrophil functions. *J. Cell Biol.* **133**, 895-910.

Mandell, K. J., Babbin, B. A., Nusrat, A. and Parkos, C. A. (2005). Junctional adhesion molecule 1 regulates epithelial cell morphology through effects on beta1 integrins and Rap1 activity. *J. Biol. Chem.* **280**, 11665-11674.

Martin-Padura, I., Lostaglio, S., Schneemann, M., Williams, L., Romano, M., Fruscella, P., Panzeri, C., Stoppacciaro, A., Ruco, L., Villa, A. et al. (1998). Junctional adhesion molecule, a novel member of the immunoglobulin superfamily that distributes at intercellular junctions and modulates monocyte transmigration. *J. Cell Biol.* **142**, 117-127.

Mempel, T. R., Moser, C., Hutter, J., Kuebler, W. M. and Krombach, F. (2003). Visualization of leukocyte transendothelial and interstitial migration using reflected light oblique transillumination in intravital video microscopy. *J. Vasc. Res.* **40**, 435-441.

Naik, M. U. and Naik, U. P. (2006). Junctional adhesion molecule-A-induced endothelial cell migration on vitronectin is integrin alpha v beta 3 specific. *J. Cell Sci.* **119**, 490-499.

Naik, M. U., Mousa, S. A., Parkos, C. A. and Naik, U. P. (2003). Signaling through JAM-1 and alphavbeta3 is required for the angiogenic action of bFGF: dissociation of the JAM-1 and alphavbeta3 complex. *Blood* **102**, 2108-2114.

Newburger, P. E., Chovaniec, M. E., Greenberger, J. S. and Cohen, H. J. (1979). Functional changes in human leukemic cell line HL-60. A model for myeloid differentiation. *J. Cell Biol.* **82**, 315-322.

Ostermann, G., Weber, K. S., Zernecke, A., Schroder, A. and Weber, C. (2002). JAM-1 is a ligand of the beta(2) integrin LFA-1 involved in transendothelial migration of leukocytes. *Nat. Immunol.* **3**, 151-158.

Ostermann, G., Fraemohs, L., Baltus, T., Schober, A., Lietz, M., Zernecke, A., Liehn, E. A. and Weber, C. (2005). Involvement of JAM-A in mononuclear cell recruitment on inflamed or atherosclerotic endothelium: inhibition by soluble JAM-A. *Arterioscler. Thromb. Vasc. Biol.* **25**, 729-735.

Pierini, L. M., Lawson, M. A., Eddy, R. J., Hendey, B. and Maxfield, F. R. (2000). Oriented endocytic recycling of alpha5beta1 in motile neutrophils. *Blood* **95**, 2471-2480.

Ridley, A. J., Schwartz, M. A., Burridge, K., Firtel, R. A., Ginsberg, M. H., Borisy, G., Parsons, J. T. and Horwitz, A. R. (2003). Cell migration: integrating signals from front to back. *Science* **302**, 1704-1709.

Rowin, M. E., Whatley, R. E., Yednock, T. and Bohnsack, J. F. (1998). Intracellular calcium requirements for β1 integrin activation. *J. Cell. Physiol.* **175**, 193-202.

Self, A. J., Caron, E., Paterson, H. F. and Hall, A. (2001). Analysis of R-Ras signaling pathways. *J. Cell Sci.* **114**, 1357-1366.

Tomaselli, K. J., Damsky, C. H. and Reichardt, L. F. (1988). Purification and characterization of mammalian integrins expressed by a rat neuronal cell line (PC12): evidence that they function as alpha/beta heterodimeric receptors for laminin and type IV collagen. *J. Cell Biol.* **107**, 1241-1252.

Tran, H., Pankov, R., Tran, S. D., Hampton, B., Burgess, W. H. and Yamada, K. M. (2002). Integrin clustering induces kinectin accumulation. *J. Cell Sci.* **115**, 2031-2040.

Vestweber, D. (2007). Adhesion and signaling molecules controlling the transmigration of leukocytes through endothelium. *Immunol. Rev.* **218**, 178-196.

Weber, C., Fraemohs, L. and Dejana, E. (2007). The role of junctional adhesion molecules in vascular inflammation. *Nat. Rev. Immunol.* **7**, 467-477.

Williams, L. A., Martin-Padura, I., Dejana, E., Hogg, N. and Simmons, D. L. (1999). Identification and characterisation of human junctional adhesion molecule (JAM). *Mol. Immunol.* **36**, 1175-1188.

Woodfin, A., Reichel, C. A., Khandoga, A., Corada, M., Voisin, M. B., Scheiermann, C., Haskard, D. O., Dejana, E., Krombach, F. and Nourshargh, S. (2007). JAM-A mediates neutrophil transmigration in a stimulus-specific manner in vivo: evidence for sequential roles for JAM-A and PECAM-1 in neutrophil transmigration. *Blood* **110**, 1848-1856.

Worthylake, R. A., Lemoine, S., Watson, J. M. and Burridge, K. (2001). RhoA is required for monocyte tail retraction during transendothelial migration. *J. Cell Biol.* **154**, 147-160.